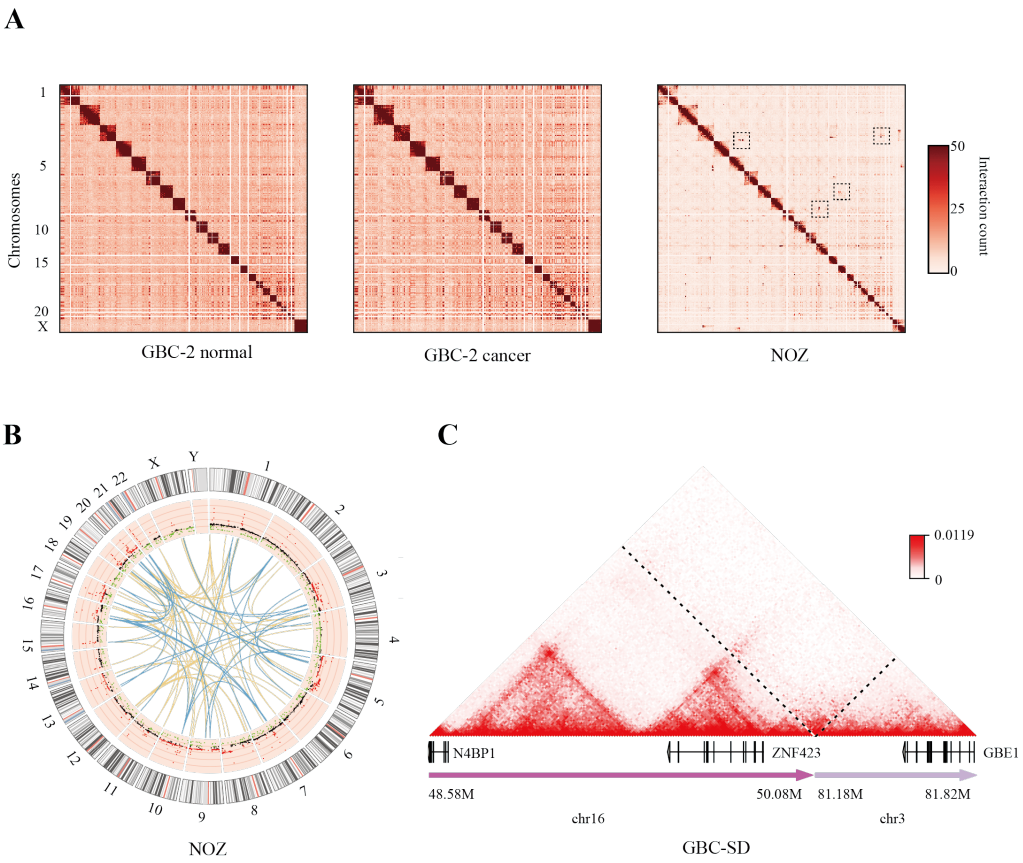

Figure S1. Whole genome interaction map and translocation events. (A) Heatmap of the contact matrices of gallbladder tissues from GBC-2 patient and GBC cell lines (NOZ) at 1 Mb resolution. The horizontal and vertical axes represent the chromosome position, and the color depth denote the intensity of interaction. Inserted black rectangles indicate strong interchromosomal interactions. (B) The 100 highest interchromosomal interactions in NOZ cells. Lines: top 100 highest interactions, blue lines: the inter- chromosome interactions overlapped with translocation events identified by WGS data. The scatter plot: CNV data, red: Integer copy numbers > 2, black: = 2, green: < 2. (C) ZNF423 genes affected by

translocation events in the junction region of rearranged genome fragments by NeoLoopFinder.

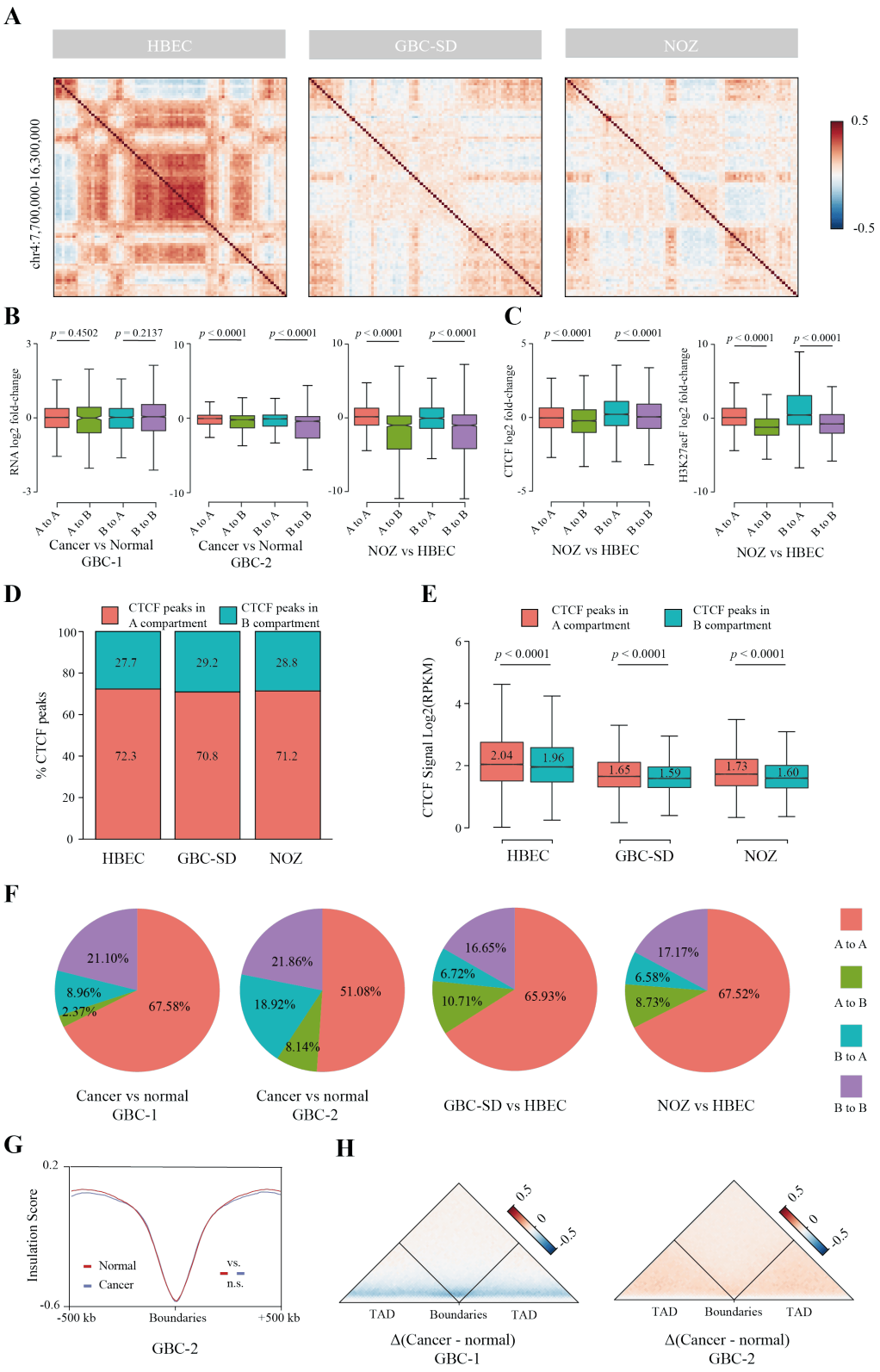

Figure S2. Compartment and TAD reorganizations in GBC. (A) An example of

compartment switches at chromosome 4 in GBC-SD and NOZ cells compared with HBECs. (B) Gene expression changes in four types of genomic compartment switches. (C) Changes in CTCF and H3K27ac ChIP-seq signal in four types of genomic compartment switches in NOZ vs. HBEC. (D) Percentage of CTCF peaks distribution in A/B compartments. (E) The CTCF ChIP-seq signal (log2RPKM) in A or B compartments. (F) Pie charts showed the distribution of differential expression genes among four types of compartment switches. (G) The average insulation score in tissue samples (GBC-2) at the 500 kb flank of boundaries. (H) Alterations of inter-TAD and intra-TAD interactions detected in GBC-1 and GBC-2 tumor tissues compared to normal tissue.

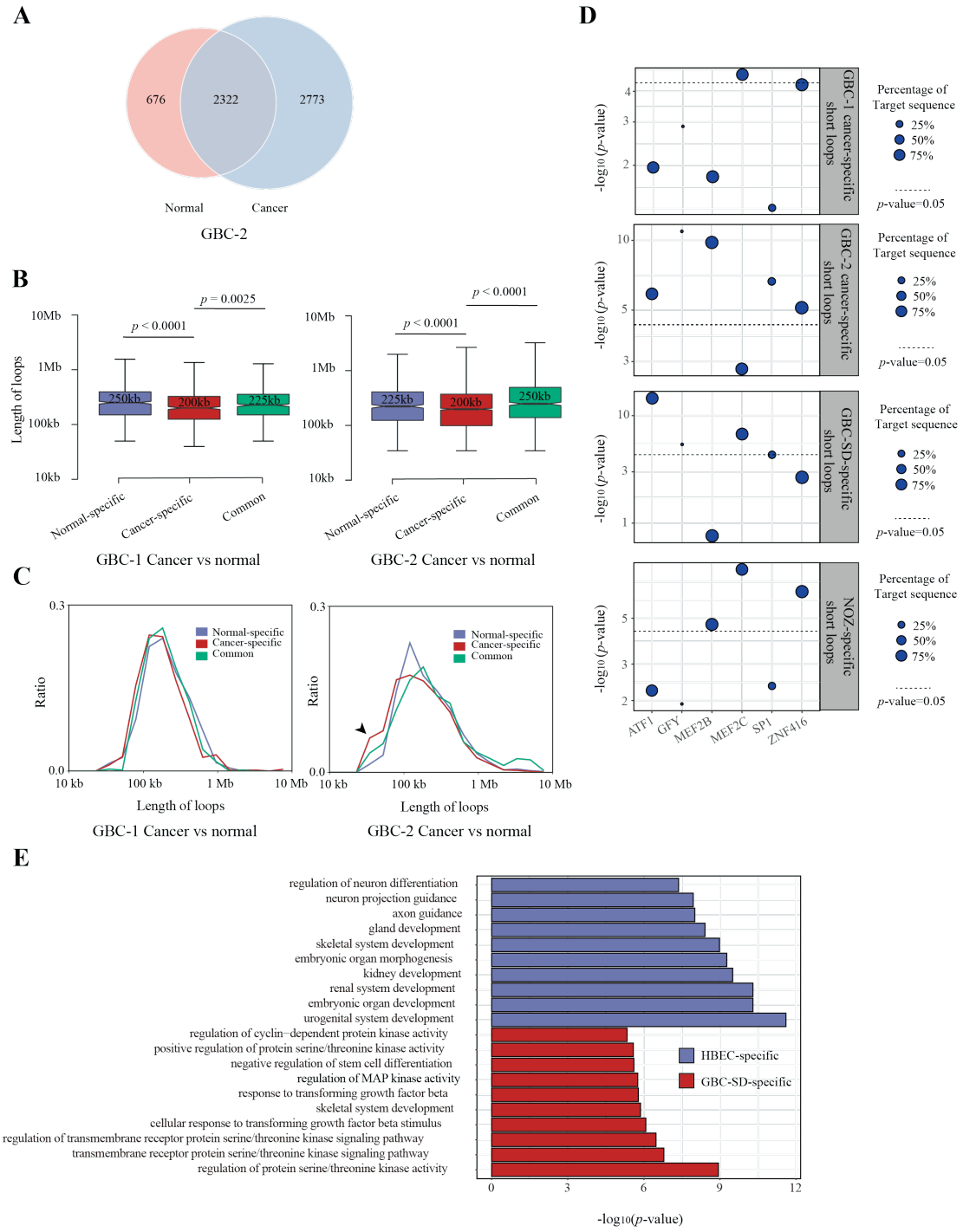

Figure S3. Characteristics of loops in GBC. (A) Venn diagrams showed the number of

loop overlaps between GBC-2 normal tissue and cancer tissue. (B, C) Length distribution of loops (normal-specific, cancer-specific and common) in GBC-1 and GBC-2. (D) TF motifs enriched at short loop ends. Points were scaled by percentage of loop ends. (E) GO enrichment analysis of genes in the HBEC-specific loops (purple) and the GBC-SD-specific loops (red).

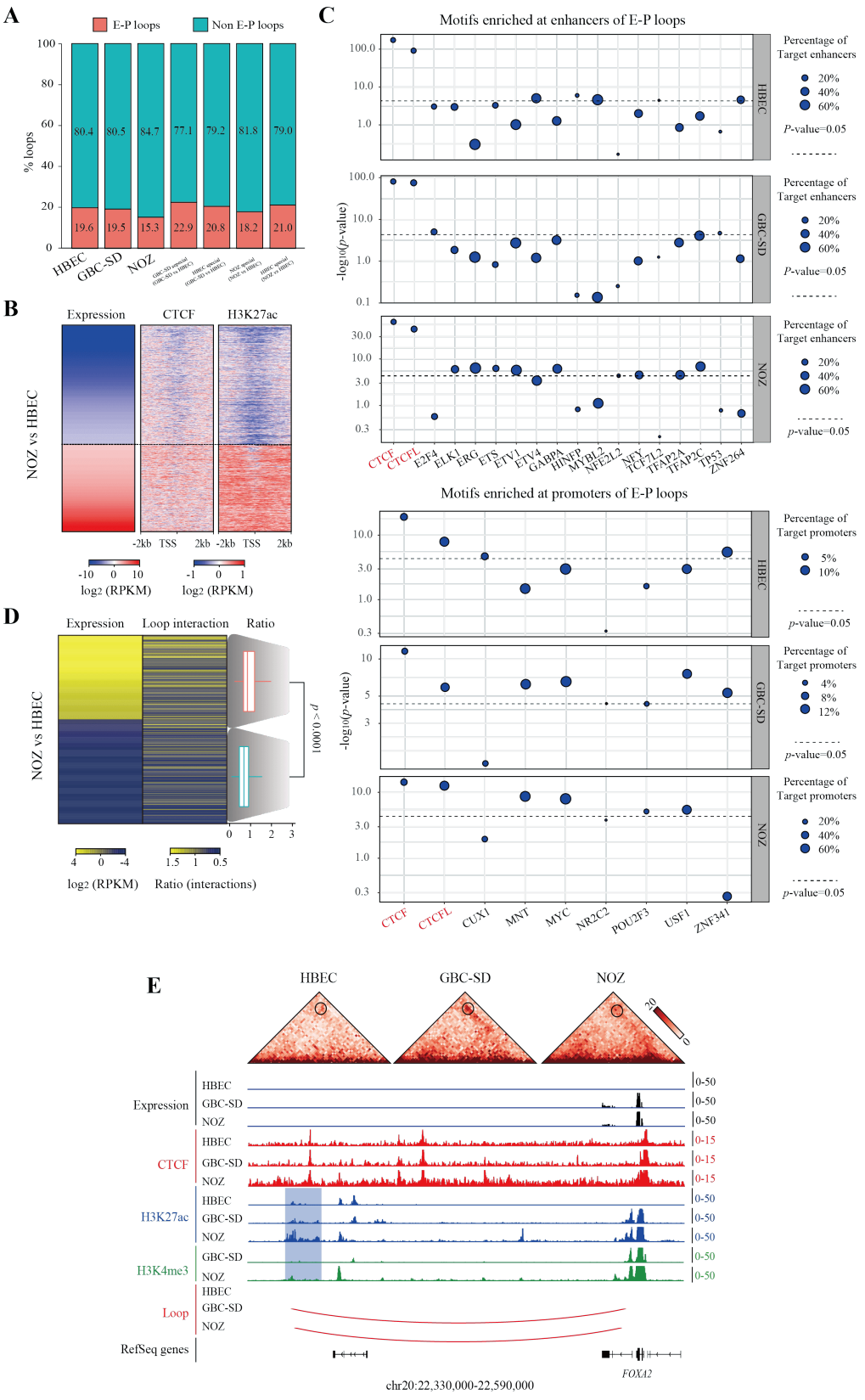

Figure S4. Relationship between CTCF, loops and gene expression. (A) Percentage of

E-P loops in total loops. (B) The heatmap represented the correlation of gene expression, CTCF and H3K27ac signal in NOZ vs. HBEC. (C) TF motifs enriched at enhancers and promoters of E-P-associated loops. Points were scaled by percentage of loops with motifs. (D) The left heatmaps represented the relative expression (NOZ vs. HBEC) of genes with E-P loops. The ratios of Hi-C interaction normalized counts involved in the E-P loops of the corresponding genes were shown on the right. (E) The Hi-C heatmap, gene expression, CTCF, H3K27ac and H3K4me3 signals and loops regulating FOXA2 gene.

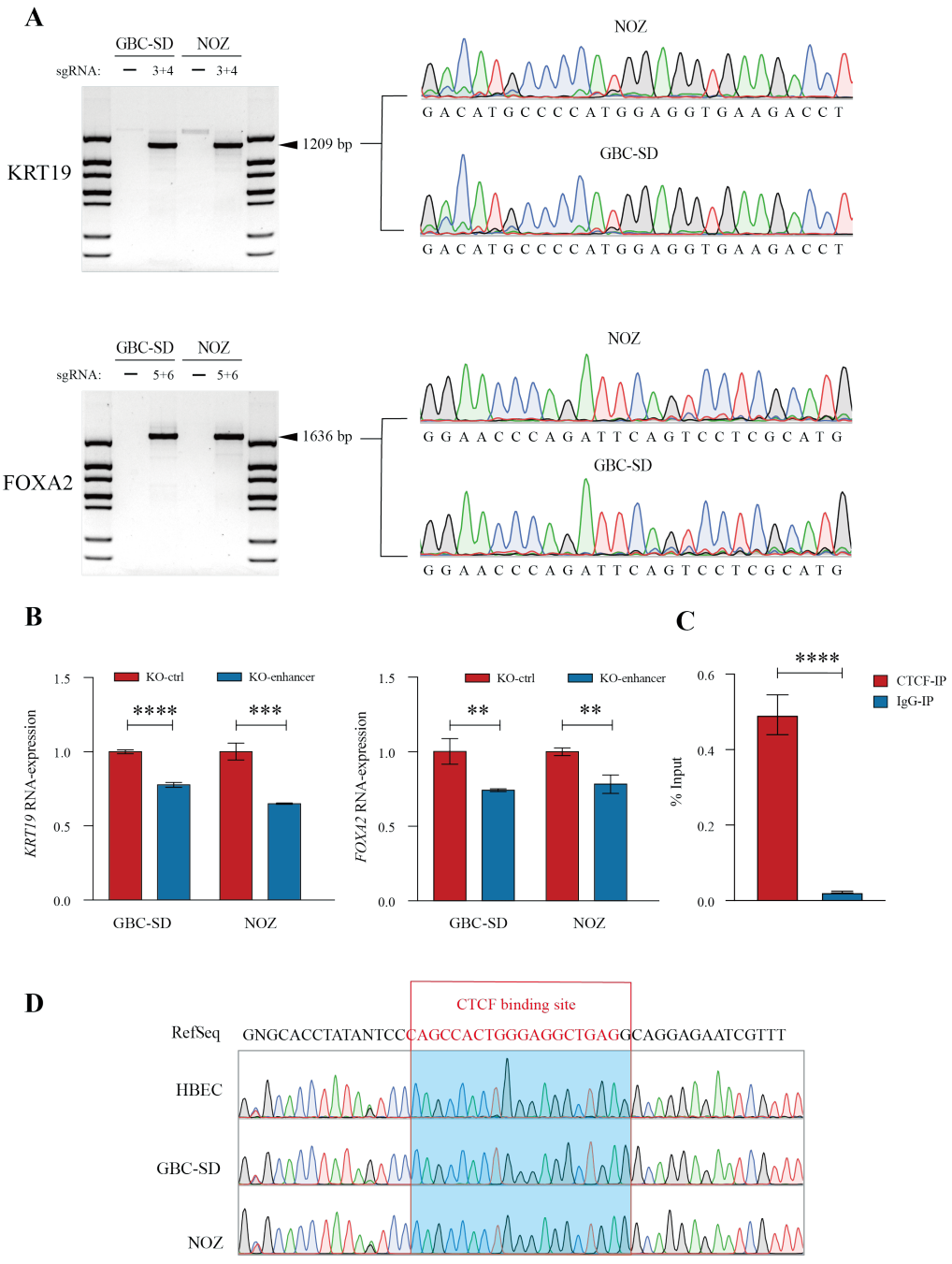

Figure S5. Deletion of candidate enhancer led to down-regulation of KRT19 and FOXA2 expression. (A) Enhancer deletion was identified by PCR and Sanger sequence using paired primers on both sides of sgRNAs. (B) qPCR validation of reduced expression of KRT19 and FOXA2 in enhancer deleted GBC cells compared with control cell. (C) CTCF

ChIP-qPCR validation of binding of CTCF protein at downstream of putative enhancer related to BMP4. (D) Targeted Sanger sequencing indicated no mutation in the CTCF binding site.